Regina: *new challenges for REsearch on Graphene: from growth and state-of-the-art characterization towards INdustrial Applications*

Adriatico Guesthouse, Trieste, 3-4 December 2013

Direct View of Hot Carrier Dynamics in Graphene by Time and Angular Resolved Photoelectron Spectroscopy

J. C. Johannsen[1], S. Ulstrup[2], F. Cilento[3], A. Crepaldi[3], M. Zacchigna[4], C. Cacho[5], I. C. E. Turcu[5], E. Springate[5], F. Fromm[6], C. Raidel[6], T. Seyller[6], F. Parmigiani[3,7], M. Grioni[1], P. Hofmann[2].

1. Institute of Condensed Matter Physics, École Polytechnique Fédérale de Lausanne (EPFL), 1015 Lausanne, Switzerland; **2.** Department of Physics and Astronomy, Interdisciplinary Nanoscience Center (iNANO), Aarhus University, 8000 Aarhus C, Denmark; **3.** Elettra – Sincrotrone Trieste S.C.p.A., 34149 Basovizza, Trieste, Italy; **4.** IOM-CNR Laboratorio TASC, Area Science Park, 34012 Trieste, Italy; **5.** Central Laser Facility, STFC Rutherford Appleton Laboratory, Didcot OX11 0QX, United Kingdom; **6.** Institut für Physik, Technische Universität Chemnitz, 09126 Chemnitz, Germany; **7.** Department of Physics, University of Trieste, 34127 Trieste, Italy.

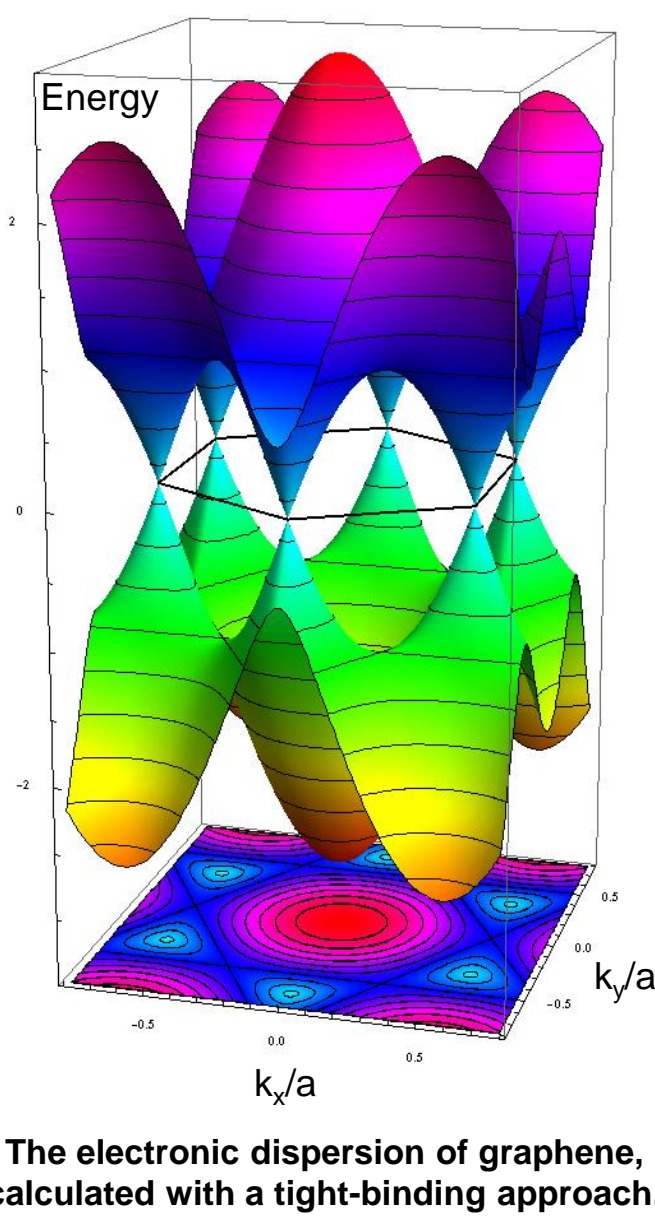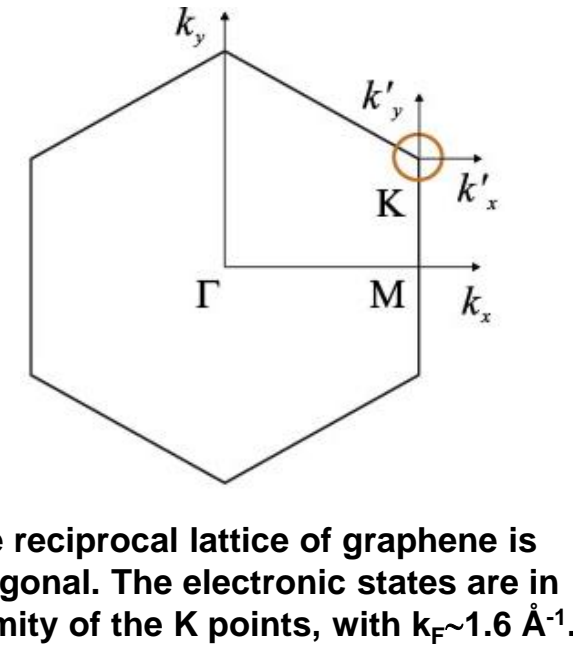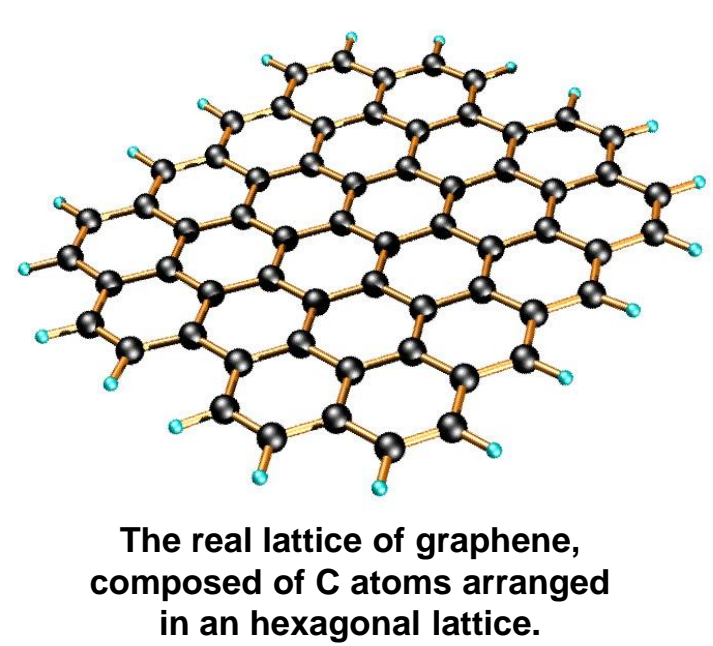## Introduction, Theory and Motivation

Graphene is one of the crystalline forms of carbon, together with graphite, carbon nanotubes, fullerenes and diamond. In this material, carbon atoms are arranged in a regular hexagonal pattern, forming a perfect bi-dimensional system. Indeed, graphene can be described as a one-atom thick layer of the layered mineral graphite. High-quality graphene is very strong, light, nearly transparent, and is an excellent conductor of both heat and electricity: it is among the strongest material ever tested (100 times more than a steel film of the same thickness), has a phonon-dominated thermal conductivity and is the material displaying the lower electrical resistivity at room temperature (~10^{-6} Ωcm). Graphene is thus emerging as a premier material for present and future technological applications, including electrical, electronic, medical and chemical ones. Its perfect bidimensionality leads to a wealth of unique properties.

All these properties arise from the peculiar electronic structure, characterized by a linear dispersion relation for electrons and holes, described by the Dirac equation: $E = hv_F\sqrt{k_x^2 + k_y^2}$, with v_F~10^6 m/s. This relation holds at low energies near the six corners of the two-dimensional hexagonal Brillouin Zone (BZ), leading to zero effective mass for electrons and holes near the Fermi level. Because of the linear dispersion, electrons and holes at the 6 points of the k-space (at the Fermi surface) behave like relativistic particles described by the Dirac equation. Hence, the electrons and holes are called Dirac Fermions and the six corners of the BZ are called the Dirac Points (DP).

Motivated by the fact that exploiting the unique properties of graphene in electronic or optoelectronic devices inevitably involves the generation of hot carriers, i.e., electrons or holes with high energies compared to the Fermi energy, we study in detail the mechanism determining the energy transfer among the different degrees of freedom of the material, namely, electron and phonons.

To this aim, we chose an out-of-equilibrium approach, under the form of the Time and Angular Resolved Photoelectron Spectroscopy (TR-ARPES), in order to characterize how the extra energy ultrafastly injected in the system relaxes toward the phonon bath. Indeed, TR-ARPES directly reveals how the electronic distribution is modified after extra energy is absorbed by the material.

The large BZ of graphene requires using high energy photons (hv>16 eV) in order to probe the electronic band structure in the vicinity of the DPs. Hence, we performed time-resolved experiments at the ARTEMIS HHG facility (Didcot, STFC – RAL, CLF).
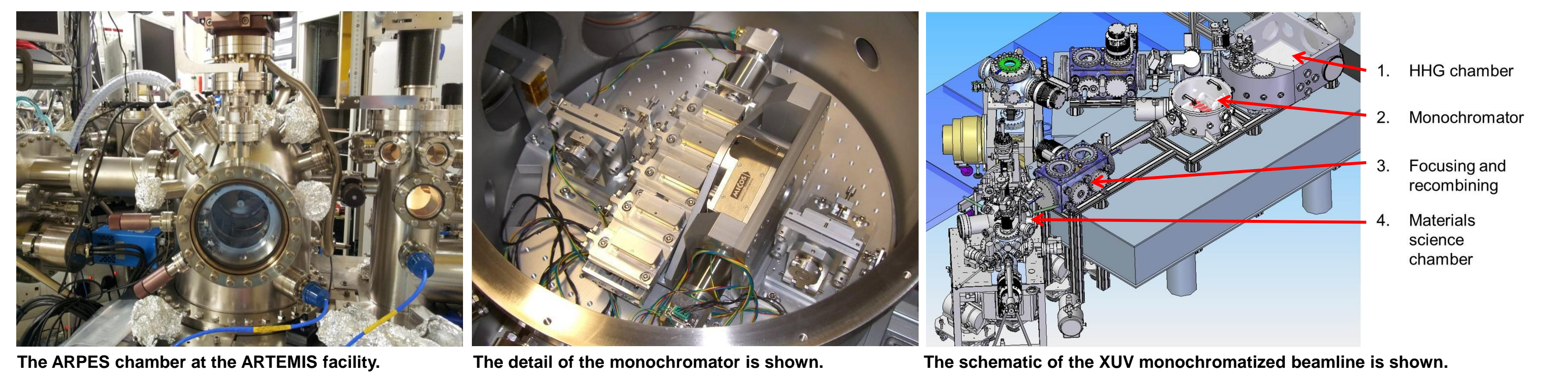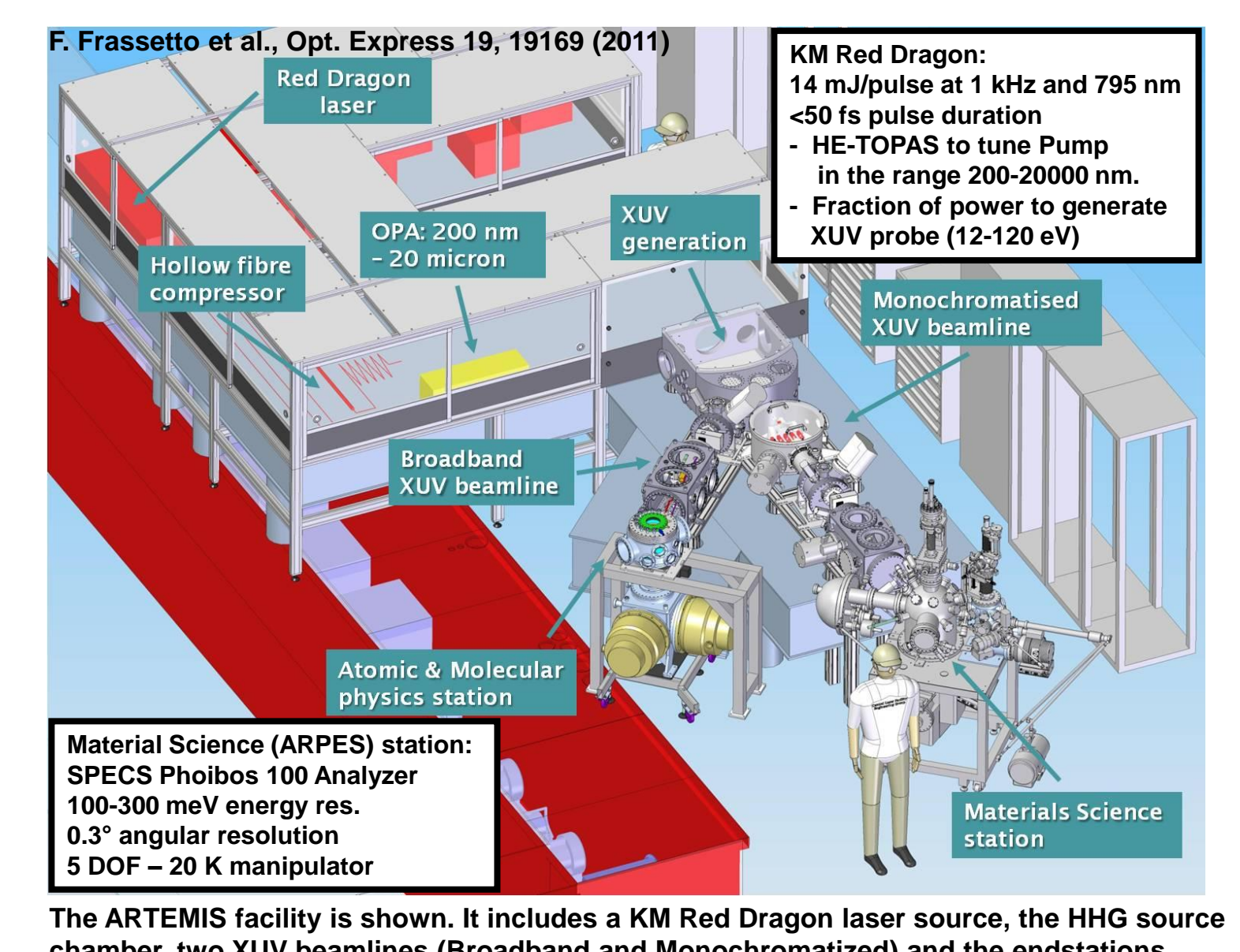
The real lattice of graphene, composed of C atoms arranged in an hexagonal lattice.

The reciprocal lattice of graphene is hexagonal. The electronic states are in proximity of the K points, with k_F~1.6 Å^{-1}.

The electronic dispersion of graphene, calculated with a tight-binding approach.

Non-Equilibrium Approach & TR-ARPES @ ARTEMIS

Out-of-Equilibrium spectroscopies with temporal resolution of ~100 fs allow to disentangle the intertwined degrees of freedom in solid state materials thanks to their different spectral features and dynamics in the non-equilibrium signal.
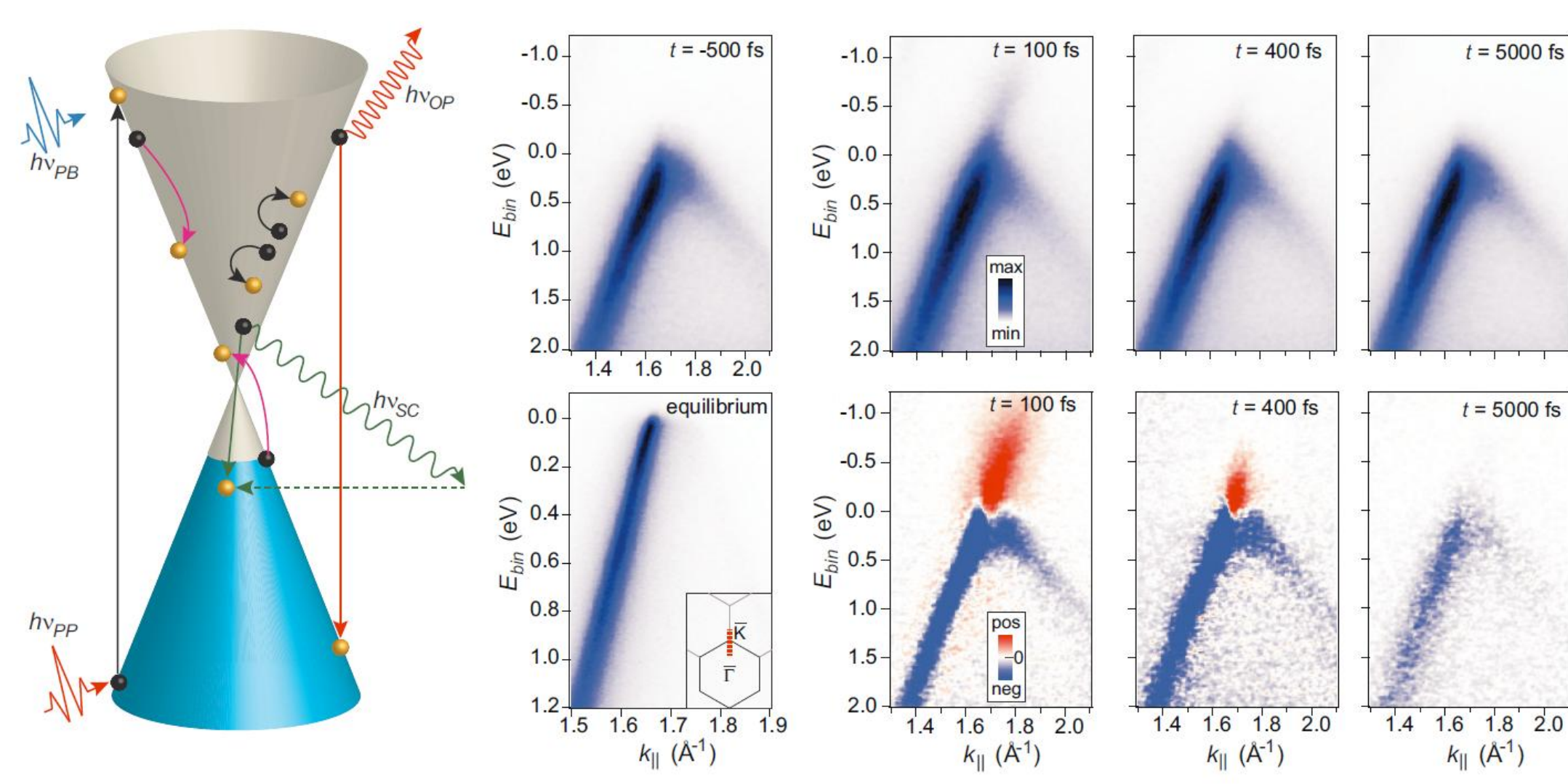
TR-ARPES provides the direct view on the evolution of the electronic structure and the electronic distribution, after the system has been brought out-of-equilibrium by the absorption of a pump pulse. At ARTEMIS, the probe beam is a tunable XUV pulse obtained by High Harmonic Generation (HHG).
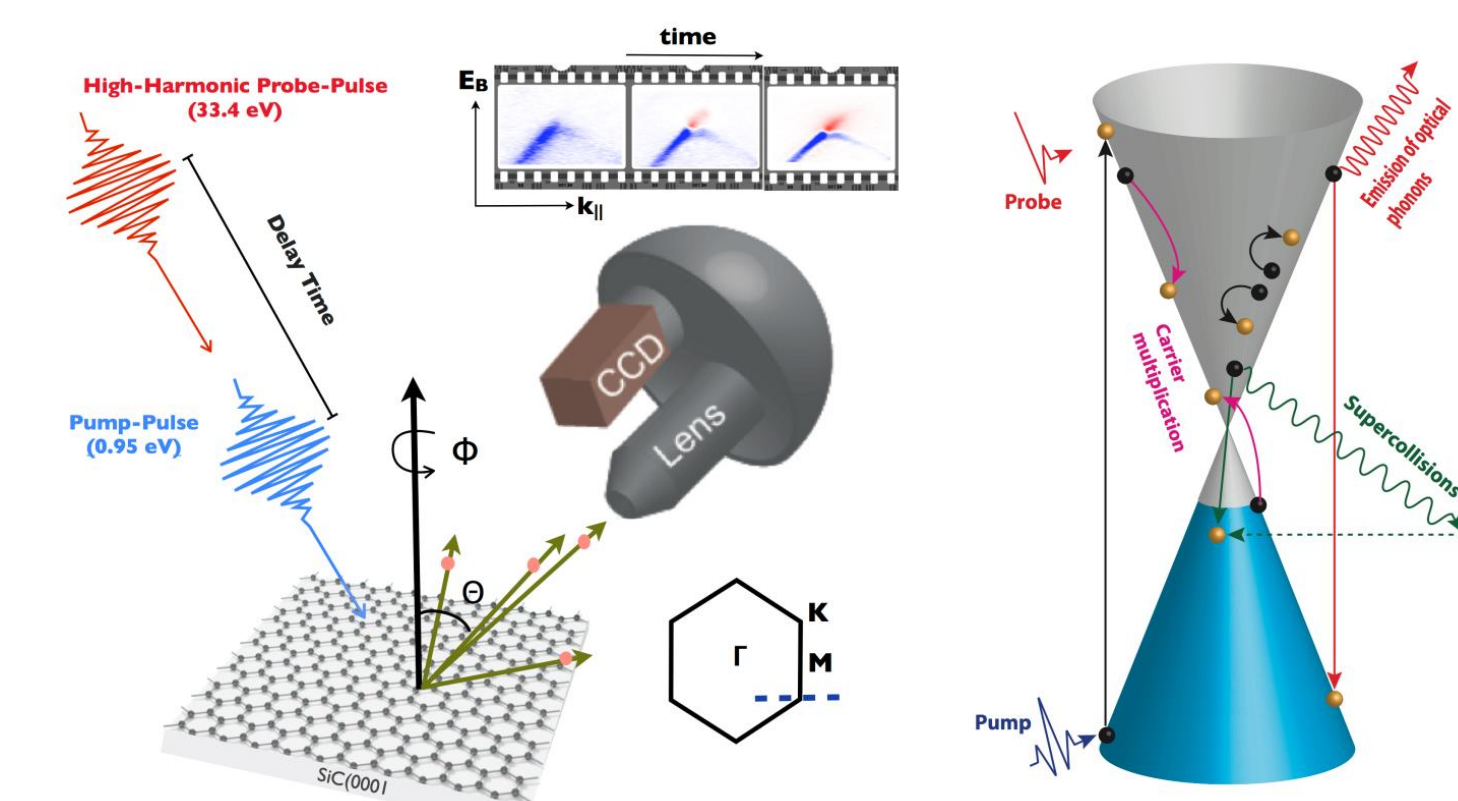
The schematic of a Pump&Probe experiment is depicted (courtesy of J.C.Johannsen). It allows to probe the evolution of the ARPES intensity as a function of the time delay (-fs) between the exciting (heating) pulse (pump, 0.95 eV) and the XUV probe pulse (33.4 eV, 21st harmonics) photoemitting electrons. The snapshot of the ARPES signal is performed by an ultrashort pulse (~50 fs), allowing to follow the relaxation dynamics. This also set the temporal resolution. On the right, the Dirac Cone and the excitation process are depicted.

F. Frassetto et al., Opt. Express 19, 19169 (2011)

KM Red Dragon:
14 mJ/pulse at 1 kHz and 795 nm
<50 fs pulse duration
- HE-TOPAS to tune Pump in the range 200-20000 nm.
- Fraction of power to generate XUV probe (12-120 eV)

Material Science (ARPES) station:
SPECS Phoibos 100 Analyzer
100-300 meV energy res.
0.3° angular resolution
5 DOF – 20 K manipulator

The ARTEMIS facility is shown. It includes a KM Red Dragon laser source, the HHG source chamber, two XUV beamlines (Broadband and Monochromatized) and the endstations.

The ARPES chamber at the ARTEMIS facility.

The detail of the monochromator is shown.

The schematic of the XUV monochromatized beamline is shown.

1. HHG chamber
2. Monochromator
3. Focusing and recombining
4. Materials science chamber

Experimental Data

The excitation mechanism across the Dirac Cone is shown. On the right, the TR-ARPES raw data collected at T=300 K are shown. Our sample is a Quasi Free Standing Monolayer Graphene (QFMG) on a SiC substrate. The Fermi level lies 240 meV below the DP. The full ARPES intensity at selected pump-probe delays is shown on the top row. On the bottom row, a high-resolution ARPES map is reported for comparison. It is acquired with a conventional ARPES setup (ASTRID- Aarhus). The differential ARPES intensity (the spectrum at t=-500 fs has been subtracted) is shown for selected pump-probe delays. Here the absorbed fluence is about 4 μJ/cm² (calculated assuming that graphene absorbs 1.3% of the incident power).
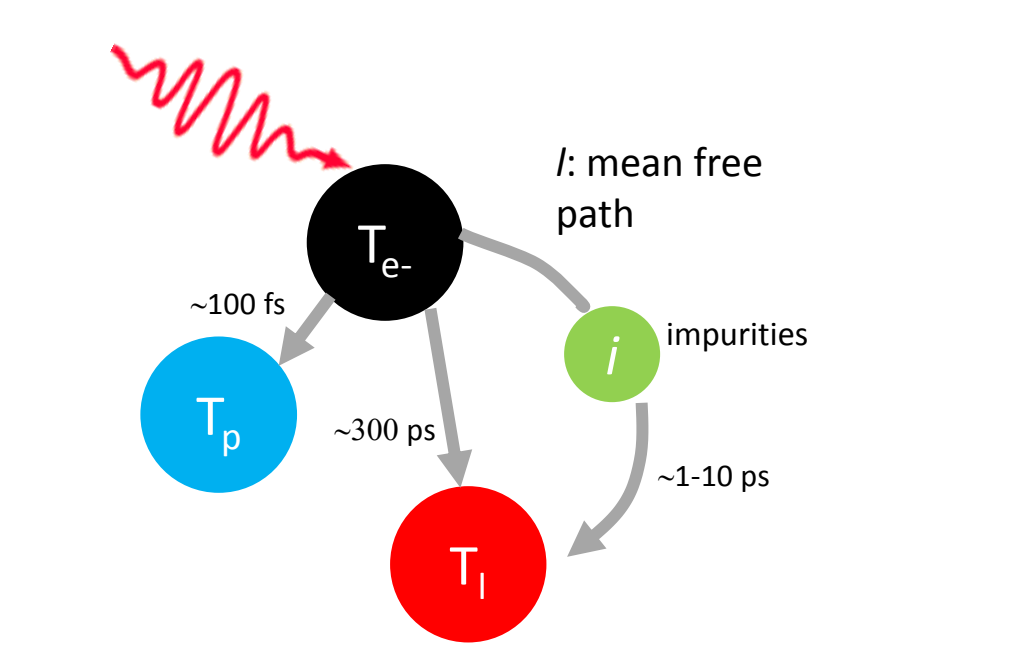
Data Analysis
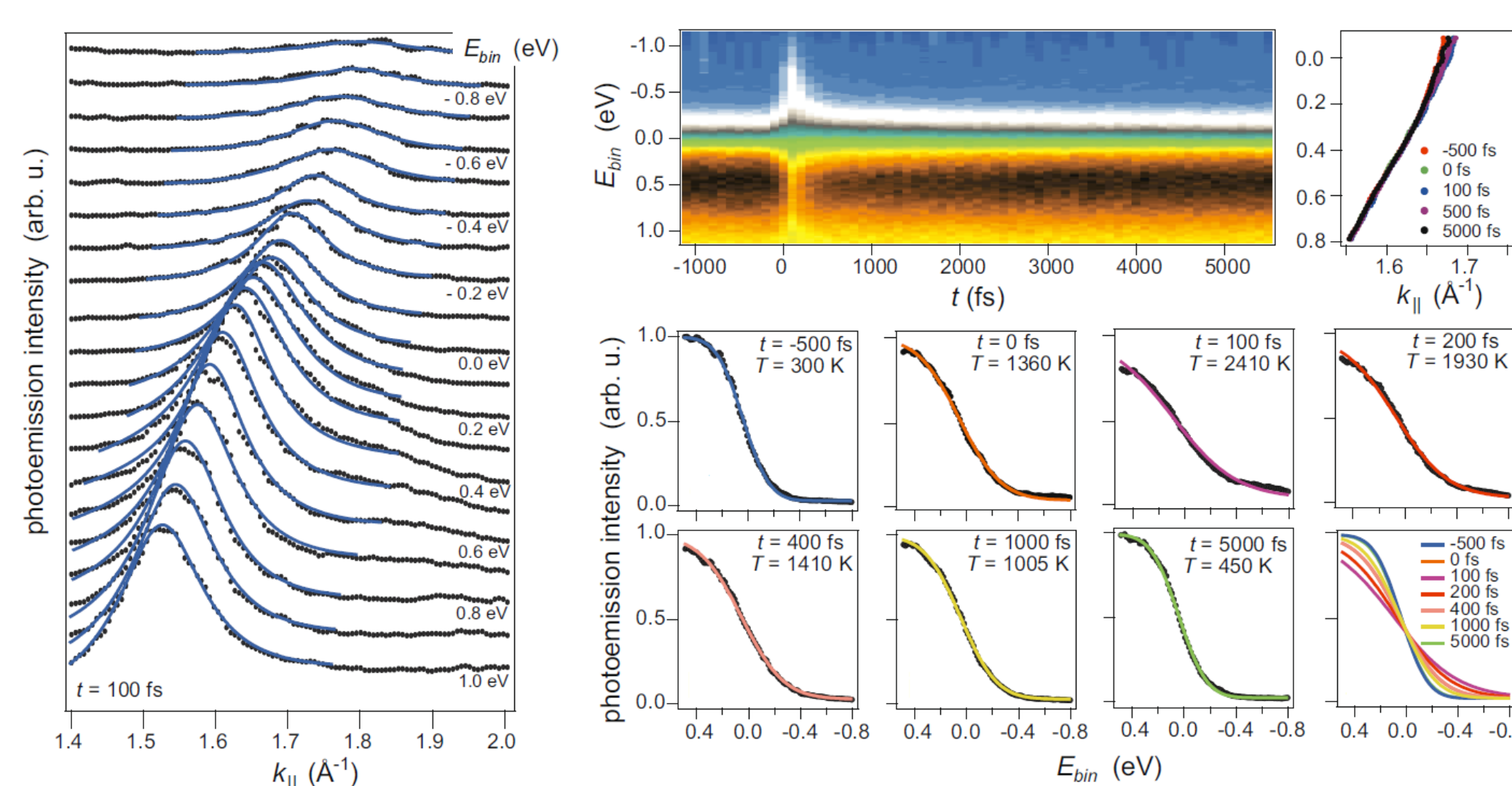
The ARPES map at t=100 fs after excitation has been sliced in MDCs. The intensity of the peak maximum as a function of energy gives a Fermi Dirac (FD) distribution. This procedure is repeated for all pump-probe delays, yielding the top graph. The FD distribution at selected delays is reported, with the result of a fitting of a FD function superimposed.
In this way, we retrieve the electronic temperature of the electrons for all pump-probe delays.

Relaxation Dynamics

τ_1~150 fs

τ_2~2500 fs

- Data
- T_e double exp. fit
- Fast Component
- Slow Component
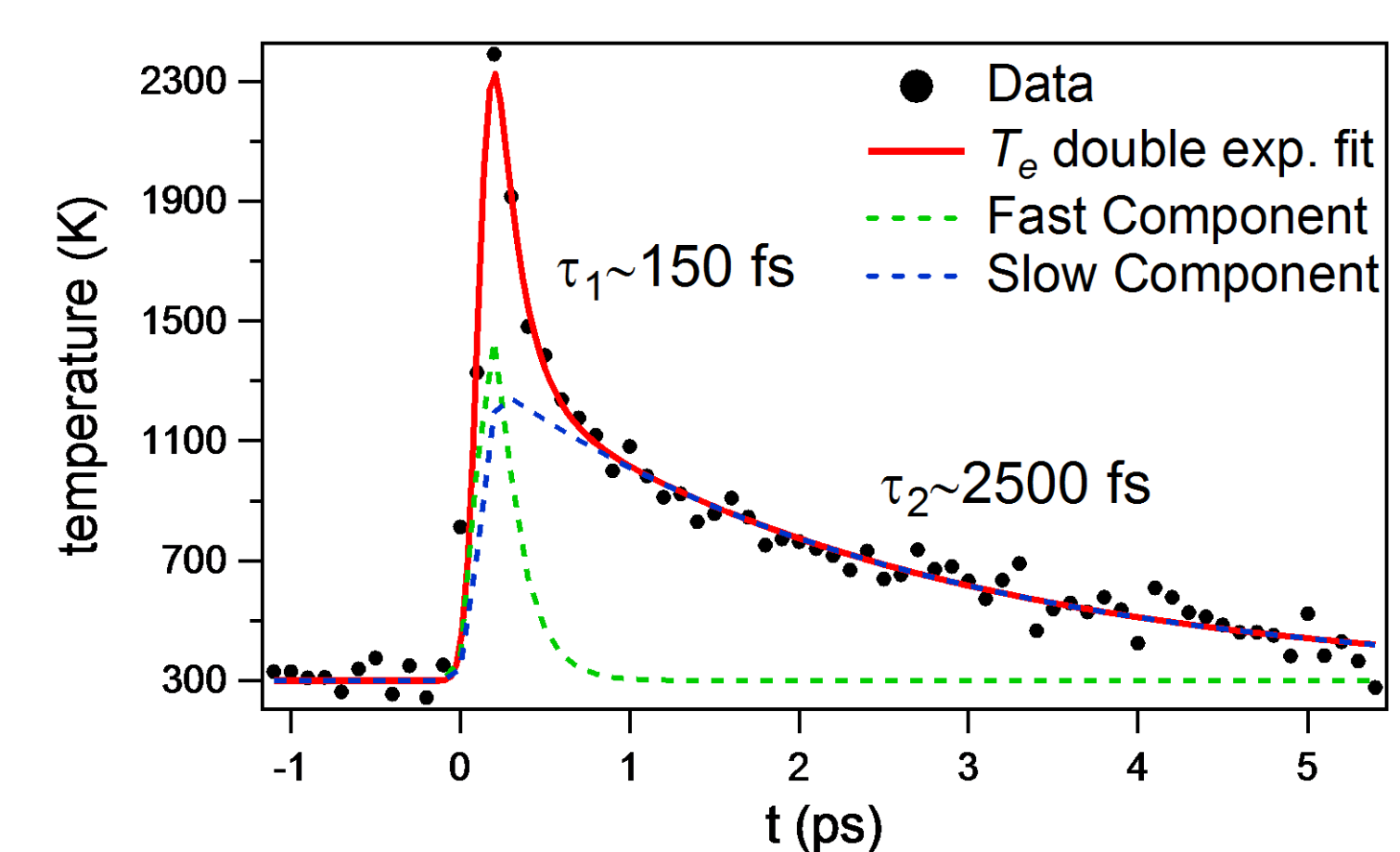
The dynamics of the electronic temperature is fitted with a sum of two exponentials (convoluted with the Gaussian experimental time resolution of ~60 fs). The result is that TWO different dynamics are clearly resolved: a fast one (that we attribute to the relaxation mediated by optical phonons), having τ_1~150 fs, and a slow one (that we attribute to the relaxation mediated by acoustic phonons), having τ_2~2500 fs.

Electron-Boson Coupling

I: mean free path

~100 fs

~300 ps

~1-10 ps

i: impurities

$$\frac{\partial T_e}{\partial t} = +\frac{S(t)}{\beta} - \frac{\pi\lambda_1 g(\mu(T_e))\Omega_{Ein}^3}{\hbar}\frac{n_e - n_p}{C_e} - 9.62\frac{\lambda_2 g(\mu(T_e))k_B^3}{\hbar k_F l}\frac{T_e^3 - T_l^3}{C_e}$$
$$- \pi\lambda_2 \hbar g(\mu(T_e))k_F^2 v_s^2 k_B \frac{T_e - T_l}{C_e},$$

$$\frac{\partial T_p}{\partial t} = \frac{C_e \pi\lambda_1 g(\mu(T_e))\Omega_{Ein}^3}{C_p}\frac{n_e - n_p}{\hbar}\frac{1}{C_e} - \frac{T_p - T_l}{\tau_p},$$

$$\frac{\partial T_l}{\partial t} = \frac{C_e}{C_l}\left(9.62\frac{\lambda_2 g(\mu(T_e))k_B^3}{\hbar k_F l}\frac{T_e^3 - T_l^3}{C_e} + \pi\lambda_2 \hbar g(\mu(T_e))k_F^2 v_s^2 k_B \frac{T_e - T_l}{C_e}\right) + \frac{C_p}{C_l}\frac{T_p - T_l}{\tau_p}$$

We make use of a "Three Temperature Model" (3TM) to model the energy flow from electrons to optical phonons (p) and acoustic phonons (l). It consists of a system of differential equations where the rate of return of the system toward equilibrium is governed solely by the coupling constants λ_1, λ_2 and the specific heats C_e, C_p, C_l. The supercollision term is included.

For further references on the 3TM, see: L. Perfetti et al., PRL 99, 197001 (2007) and S. Dal Conte et al., Science 335, 1600 (2012).
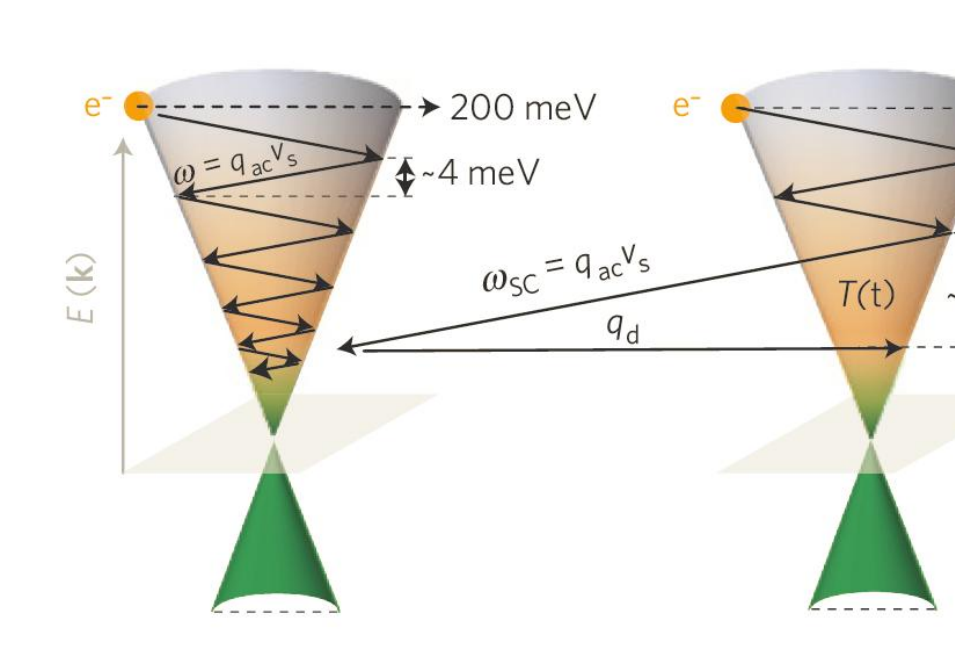
- Data
- T_e
- T_p
- T_l
- T_e (no SC)
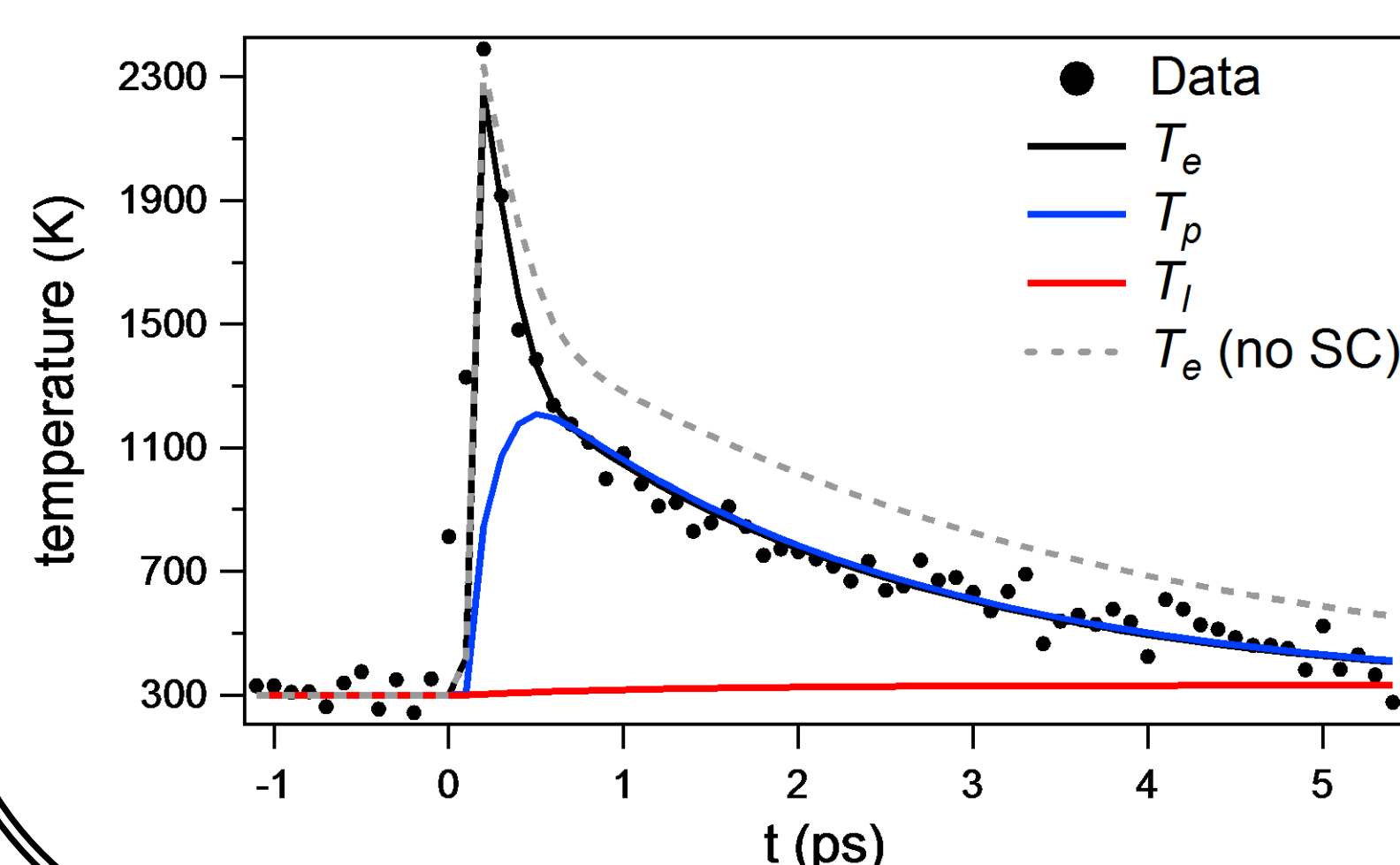
λ_1=0.033±0.007
λ_2=0.010±0.002

λ_1, λ_2 are the only free fitting parameters of the model

l, the mean free path of the electrons between defect scattering events in our sample, has been determined by high-resolution ARPES, and it results: *l*=38 Å.

Supercollisions

~ 200 meV

~4 meV

$\omega_{SC} \approx q_{ph}v_s$

$\omega_{SC} = q_{ph}v_F$

q_d

$T(t)$ ~$k_B T$

In graphene, the peculiar electronic structure at the Fermi level (Dirac Cones) and the peculiar phonon modes produce severe constraints on the relaxation processes available. Indeed, *optical phonon modes* have high energies, ~200 meV, and are available only for large energy transfers. On the contrary, *acoustic phonon modes* lies at considerably lower energies, and momentum conservation requires a huge number of scattering events in order to relax extra energy. The expected relaxation times would be of the order of several hundreds of ps. *Supercollisions*, i.e., three body scattering events involving lattice defects (the electron-phonon scattering involves scattering with an impurity) allow for large momentum transfer, thus considerably reducing the number of scattering events to achieve relaxation. Indeed, the observed cooling rate is much faster, of the order of few ps.

For more on Supercollisions:
J. Song et al., Phys. Rev. Lett. 109, 106602 (2012)
M. Graham et al., Nat ure Physics 9, 103 (2013)
A. Betz et al., Nature Physics 9, 109 (2013)

Lifetime Evolution

E_{bin} = 850 meV

- -500 fs
- 100 fs
- 400 fs
- 5000 fs

E_{bin} = 850 meV

process 1   process 2
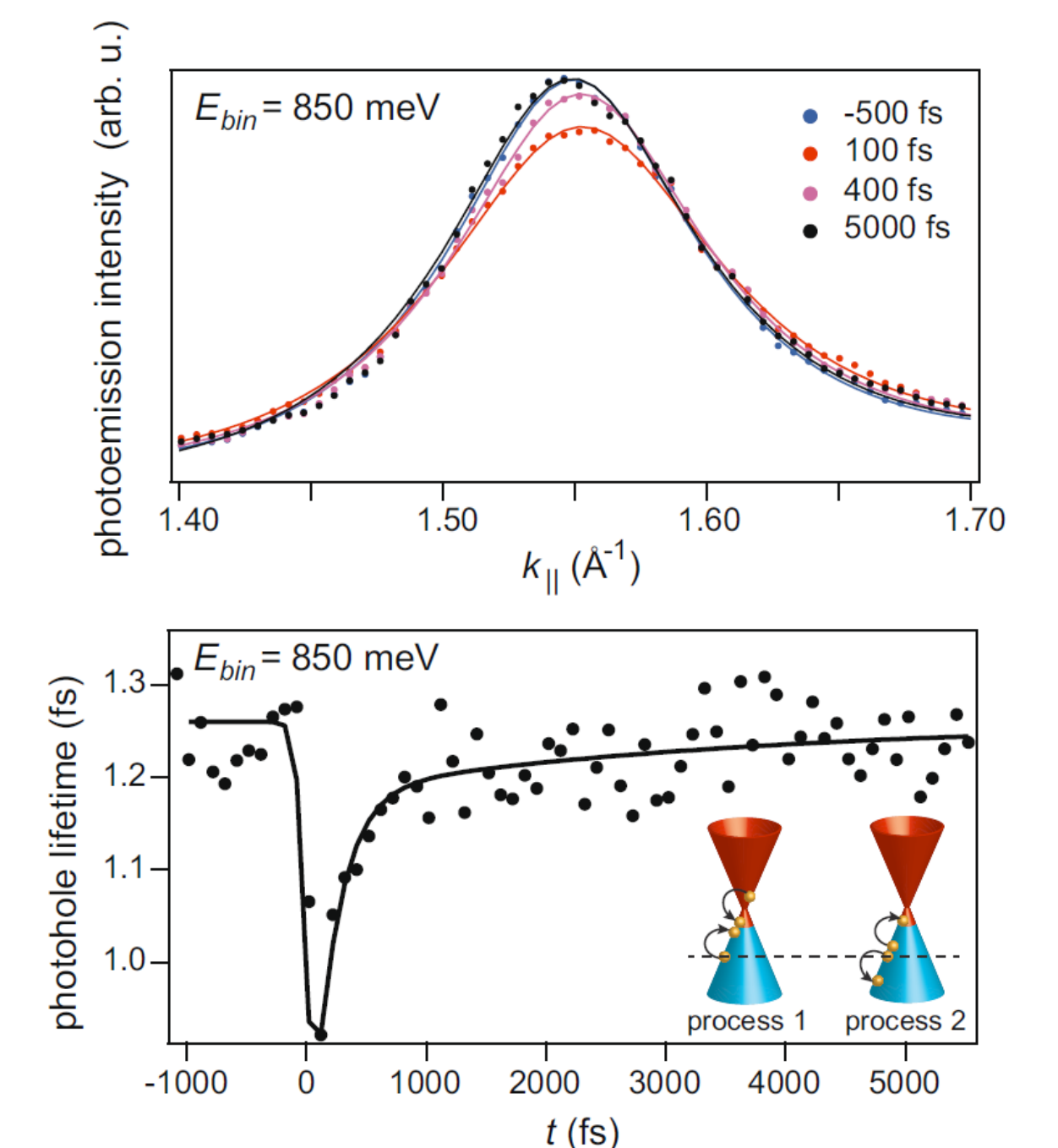
After excitation, we observe t_{max}=1.26 fs to t_{min}=0.92 fs.
A new decay channel (with t=3.5 fs) opens, and decays on a ~200 fs timescale.
We can detect this timescale, well below the experimental resolution (~60 fs), thanks to the momentum resolution and the MDC analysis.
This new timescale can result from an extra decay channel or from the temperature-dependence of the electronic scattering rate.

Conclusions

Non equilibrium spectroscopies revealed effective in order to solve a long-lasting issue in graphene, namely, the nature and strength of the electron-phonon coupling, responsible in determining the relaxation timescale of the excess energy absorbed by electrons trough different excitation mechanisms. We also pointed out that supercollisions, i.e., the scattering of electrons with phonons, mediated by impurities, constitutes a fundamental channel in the relaxation mechanism. The two lambdas, summarizing the strength of the electron-phonon coupling, result: l1=0.033, l2=0.010. Finally, we revealed an ultrafast modification of the carriers lifetime, that we interpreted as the opening of a new deexcitation channel with a lifetime of 3.5 fs, which closes on a timescale of 200 fs. The MDC analysis revealed effective in showing photoinduced alterations of the lifetime that are well below the experimental time resolution.